# Supporting Information

Tiny Ni particles dispersed in platelet SBA-15 materials induce high efficiency for $CO_2$ methanation

Ming-Han Liu[a], Ching-Shiun Chen,[*bc] Hsi-An Chen,[a] Jia-Huang Wu,[b] Hung-Chi Wu[b] and Chia-Min Yang[*a]

[a]Department of Pathology, Chang Gung Memorial Hospital, 5, Fusing St., Guishan Dist., Taoyuan City 33302, Taiwan, Republic of China.

[b]Department of Chemistry, National Tsing Hua University, Hsinchu 30013, Taiwan, Republic of China.

[c]Center for General Education, Chang Gung University, 259, Wen-Hua 1st Rd., Guishan Dist., Taoyuan City 33302, Taiwan, Republic of China.

[*]Corresponding authors

E-mail: cschen@mail.cgu.edu.tw; cmyang@mx.nthu.edu.tw

**Table S1** Comparison of $CO_2$ hydrogenation on Ni based catalysts

| Catalyst | Ni loading (wt%) | particle size (nm) | Temperature (K) | $H_2/CO_2$ ratio | GHSV ( $cm^3g^{-1}h^{-1}$) | TOF ($s^{-1}$) | $CH_4$ selectivity (%) | Reference. |
|---|---|---|---|---|---|---|---|---|
| Ni/p-SBA-15 | 3.14 | < 1 | 573 | 1/1 | 600,000 | 1.48 | 68 | this study |
| Ni/p-SBA-15 | 4.82 | 3.4 | 573 | 1/1 | 600,000 | 0.94 | 72 | this study |
| $Ni/TiO_2$ | 14.8 | 2.1 | 473 | 4/1 | 9,000 | $1.2\times10^{-3}$ | 97 | 34 |
| $Ni/TiO_2$ | 16.8 | 2.6 | 473 | 4/1 | 9,000 | $9.3\times10^{-4}$ | 99 | 34 |
| Ni@MIL-101 | 20 | 2.9 | 573 | 4/1 | 3,000 | $1.2\times10^{-3}$ | 100 | 40 |
| $Ni/CaO-Al_2O_3$ | 23 | 8.0 | 523 | 4/1 | 15,000 | $2.0\times10^{-2}$ | 90-100 | 39 |
| $Ni/SiO_2$ | 10 | 16.4 | 523 | 4/1 | 2,400 | $4.4\times10^{-3}$ | 10 | 32 |
| Ni/ZMS-5 | 10 | 14.3 | 523 | 4/1 | 2,400 | $7.6\times10^{-3}$ | 20 | 32 |
| Ni/MCM-41 | 10 | 30.3 | 523 | 4/1 | 2,400 | $3.4\times10^{-3}$ | 5 | 32 |
| $Ni/ZrO_2$ | 3 | 1.4 | 573 | 4/1 | 15,000 | $5.4\times10^{-3}$ | 100 | 50 |
| $Ni/ZrO_2$ | 6 | 2.3 | 473 | 4/1 | 15,000 | $1.2\times10^{-2}$ | 100 | 50 |
| $Ni/ZrO_2$ | 9 | 3.8 | 473 | 4/1 | 15,000 | $7.0\times10^{-3}$ | 100 | 50 |
| Ni/SBA-15 | 3 | 6.8 | 673 | 4/1 | 24,900 | 1.2 | 98 | 51 |
| Ni/SBA-15 | 5 | 7.0 | 673 | 4/1 | 24,900 | 1.63 | 99 | 51 |
| Ni/SBA-15 | 10 | 8.7 | 673 | 4/1 | 24,900 | 1.61 | 99 | 51 |
| Ni/MSN | 5 | 9.9 | 573 | 4/1 | 50,000 | 1.61 | 100 | 52 |

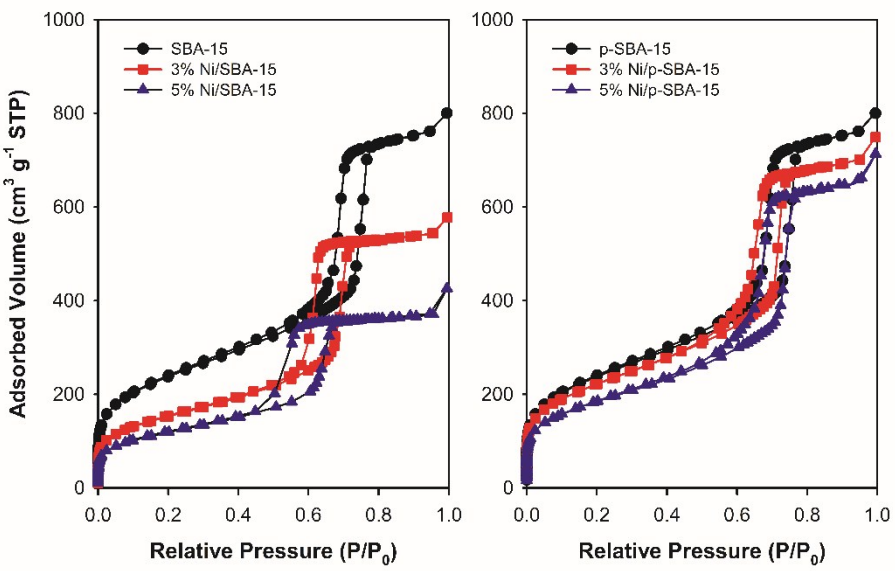


**Fig. S1** $N_2$ physisorption measurements of the p-SBA-15, SBA-15, Ni/p-SBA-15 and Ni/SBA-15 samples.

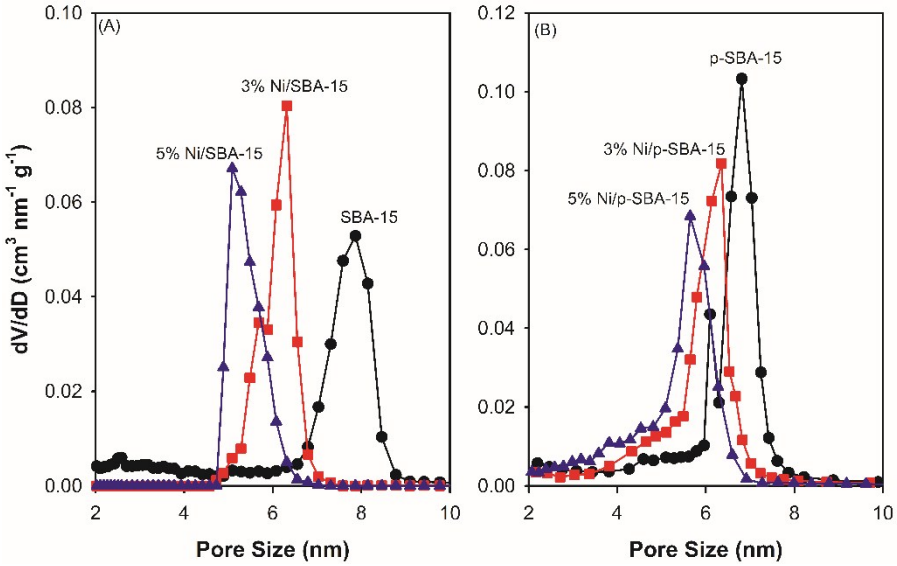


Fig. S2 The curves of pore distribution for the p-SBA-15, SBA-15, Ni/p-SBA-15 and Ni/SBA-15 samples.

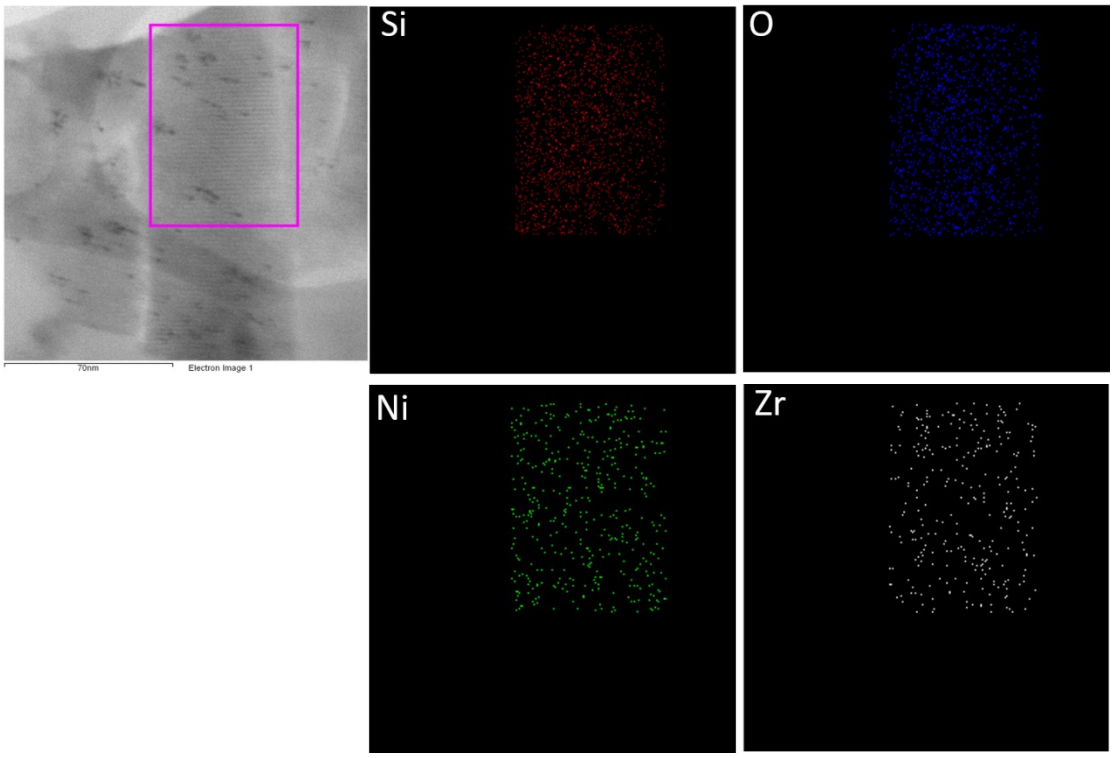


**Fig. S3** Energy-dispersive spectroscopy (EDS) of 3 wt% Ni/p-SBA-15.

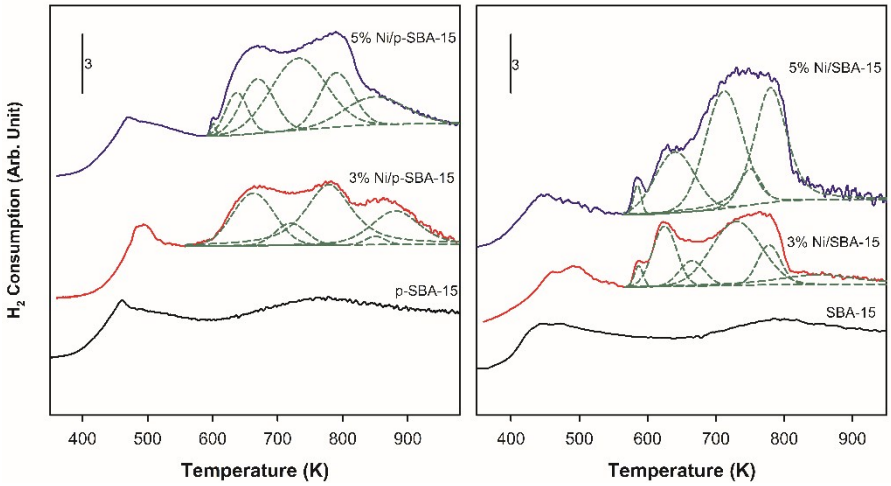


**Fig. S4** $H_2$-TPR profiles of the p-SBA-15, SBA-15, NiO/p-SBA-15 and NiO/SBA-15 samples after calcination in air at 773 K for 5 h.

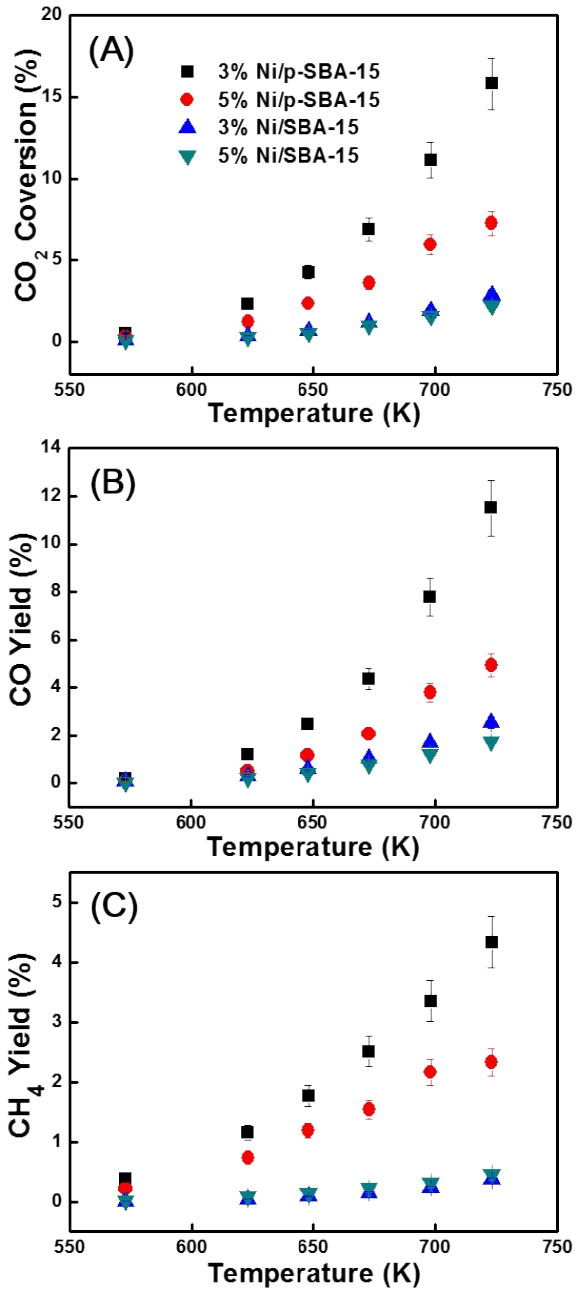


**Fig. S5** Temperature-dependent $CO_2$ hydrogenation on the Ni/p-SBA-15 and Ni/SBA-15 catalysts: (A) overall $CO_2$ conversionn; (B) CO yield and (C) $CH_4$ yield. A $H_2/CO_2$ stream (1:1 ratio) with a 100 mL $min^{-1}$ flow rate was passed over 10 mg of the catalyst. The GHSV was 600,000 $cm^3g^{-1}h^{-1}$.

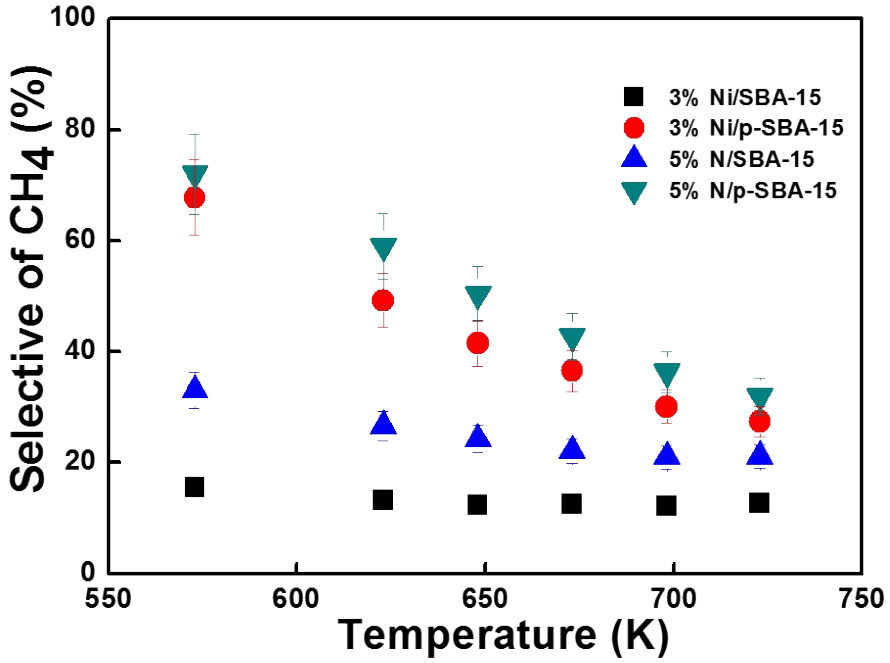


**Fig. S6** Comparison of the $CH_4$ selectivity during $CO_2$ hydrogenation on the Ni/p-SBA-15 and Ni/SBA-15 catalysts as a function of temperature.

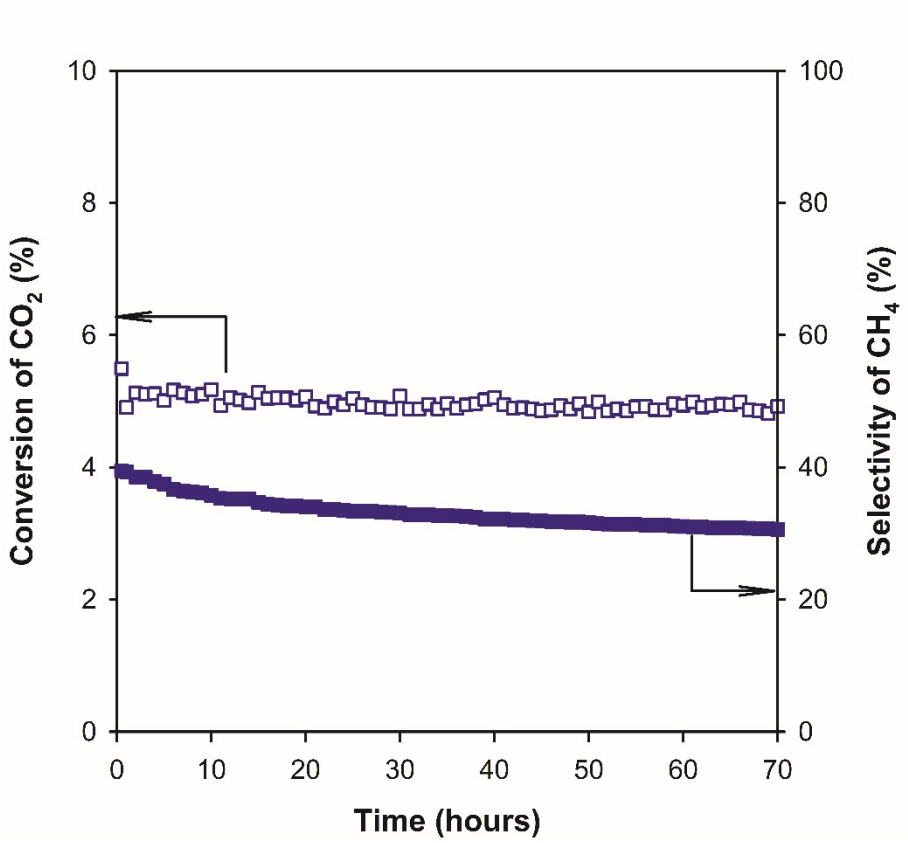


**Fig. S7** Time-dependent conversion and $CH_4$ selectivity during $CO_2$ hydrogenation on the 3 wt% Ni/ SBA-15 catalyst. A $H_2/CO_2$ stream (1:1 ratio) with a 100 mL $min^{-1}$ flow rate was passed over the catalyst.

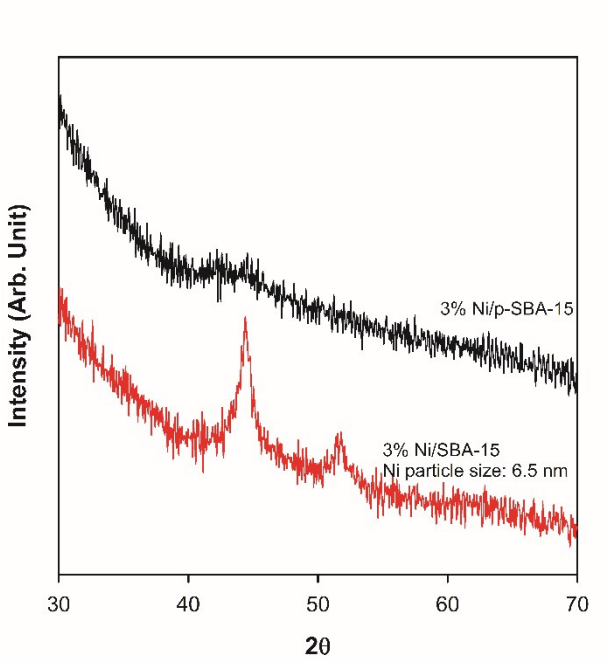


Fig. S8 XRD spectra of 3 wt% Ni/p-SBA-15 and 3 wt% Ni/SBA-15 catalysts after the long-term tests in Fig. 7 and Fig. S7.

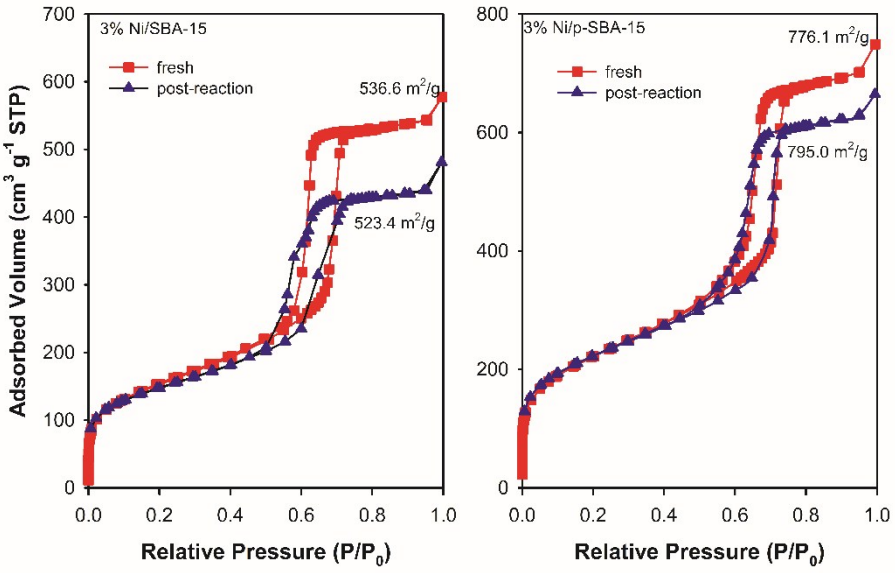


Fig. S9 $N_2$ physisorption measurements of the fresh and post-reaction for 3 wt% Ni/p-SBA-15 and 3 wt% Ni/SBA-15 catalysts.

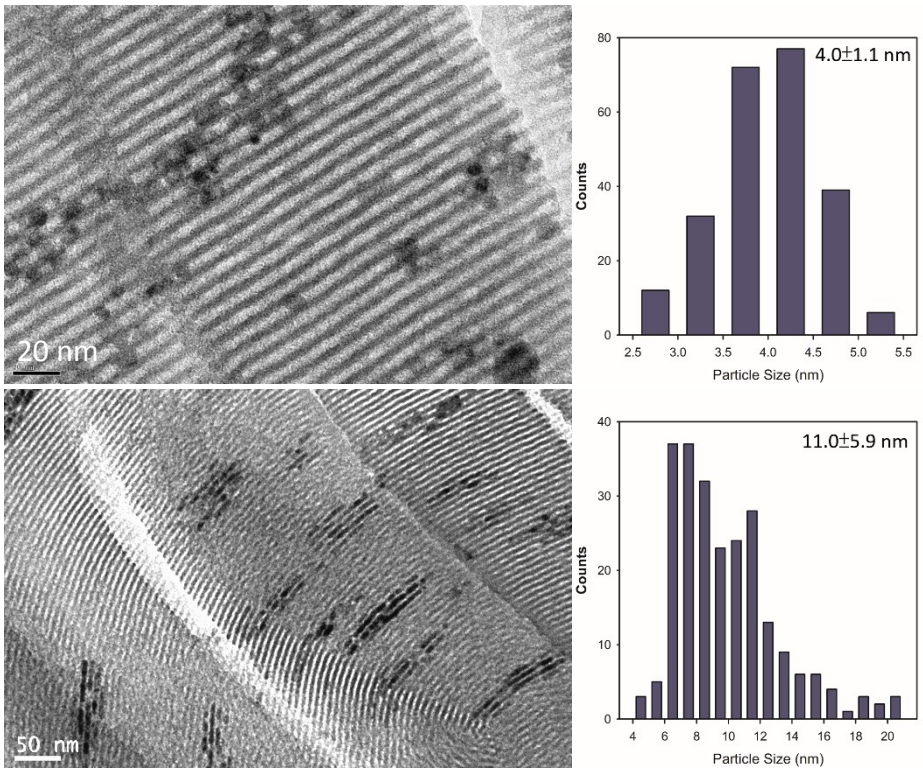


Fig. S10 TEM and particle distribution of the fresh and post-reaction for 3 wt% Ni/p-SBA-15 and 3 wt% Ni/SBA-15 catalysts.

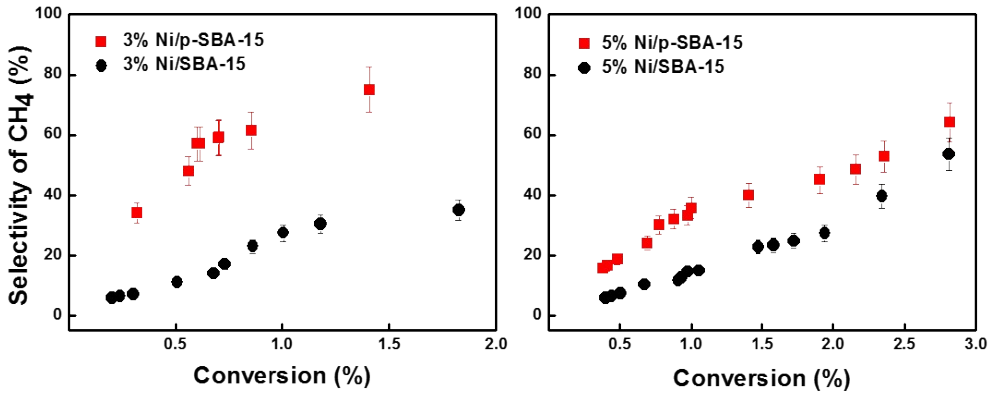


**Fig. S11** Comparison of the $CH_4$ selectivity versus reaction conversion on the Ni/p-SBA-15 and Ni/SBA-15 catalysts at 573 K.

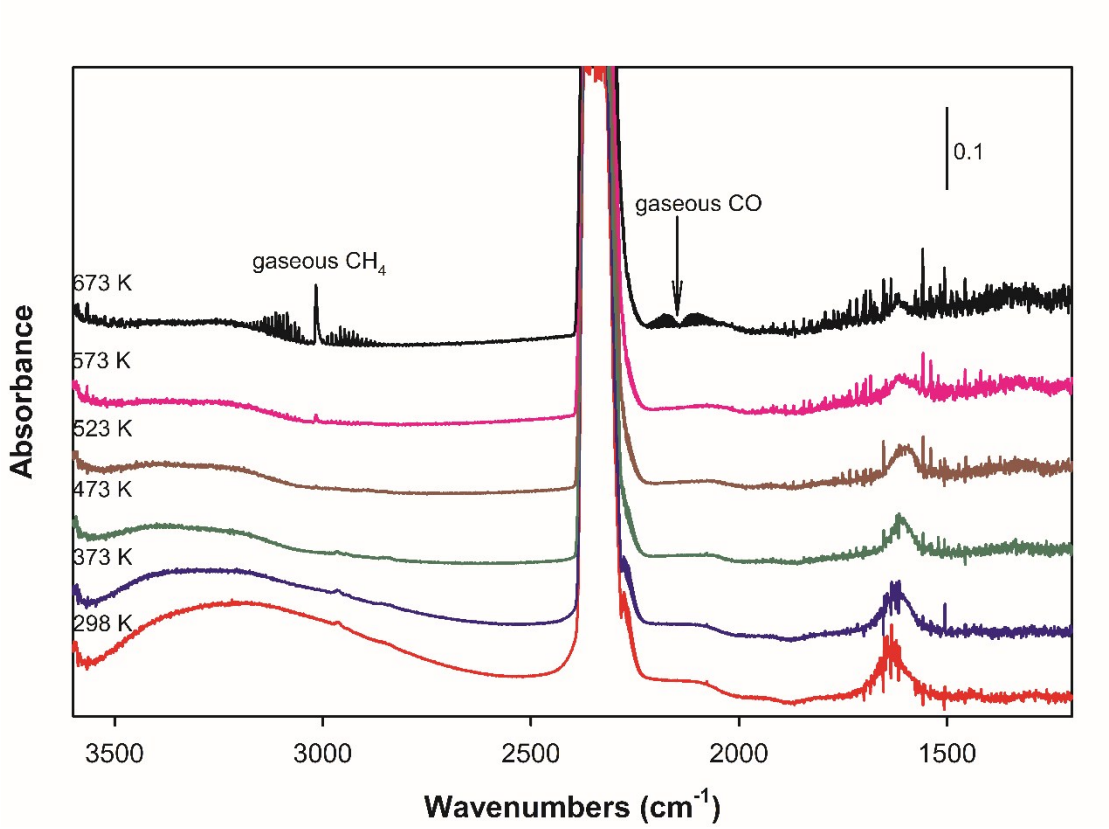


**Fig. S12** IR spectra of $H_2$ and $CO_2$ coadsorbed onto the 3 wt% Ni/SBA-15 catalyst at various temperatures. A $H_2/CO_2$ (50/50) stream with a 20 mL $min^{-1}$ flow rate was passed over the catalyst.

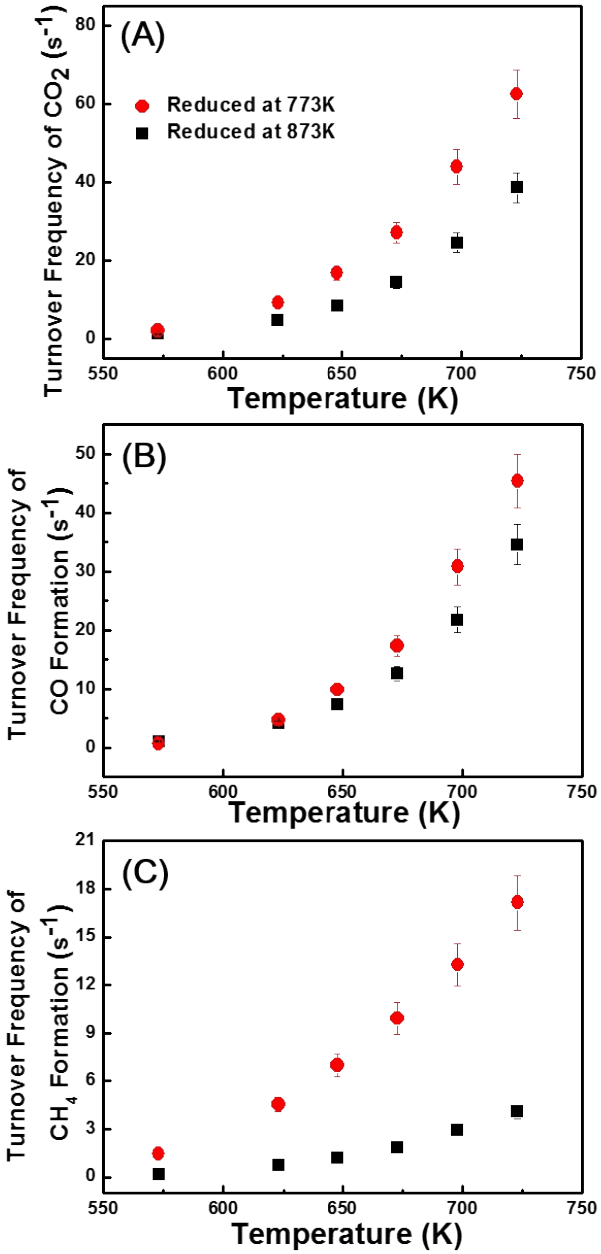


Fig. S13 Temperature-dependent reaction rates for $CO_2$ hydrogenation on the different reduction temperature on 3 wt% Ni/p-SBA-15: (A) overall $CO_2$ hydrogenation; (B) CO formation and (C) $CH_4$ formation. A $H_2/CO_2$ stream (1:1 ratio) with a 100 mL $min^{-1}$ flow rate was passed over 10 mg of the catalyst. The GHSV was 600,000 $cm^3g^{-1}h^{-1}$.

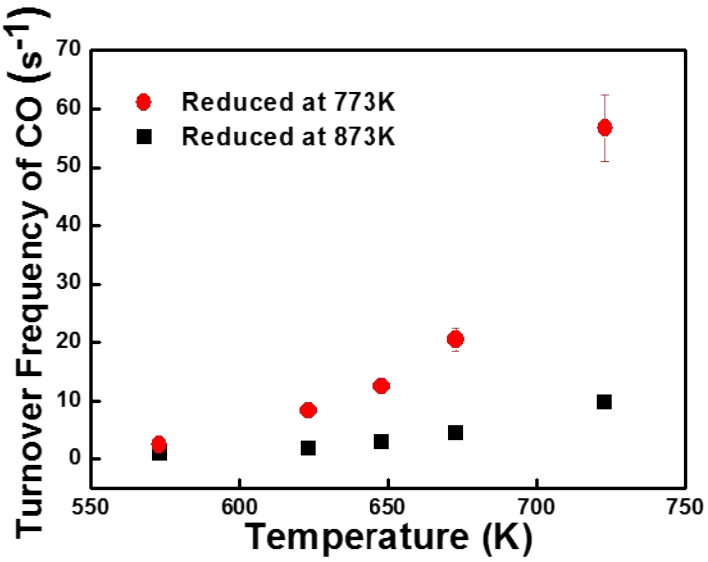


Fig. S14 Temperature-dependent reaction rates for CO hydrogenation on the different reduction temperature on 3 wt% Ni/p-SBA-15. A $H_2$/CO stream (3:1 ratio) with a 100 mL $min^{-1}$ flow rate was passed over 10 mg of the catalyst. The GHSV was 600,000 $cm^3g^{-1}h^{-1}$.

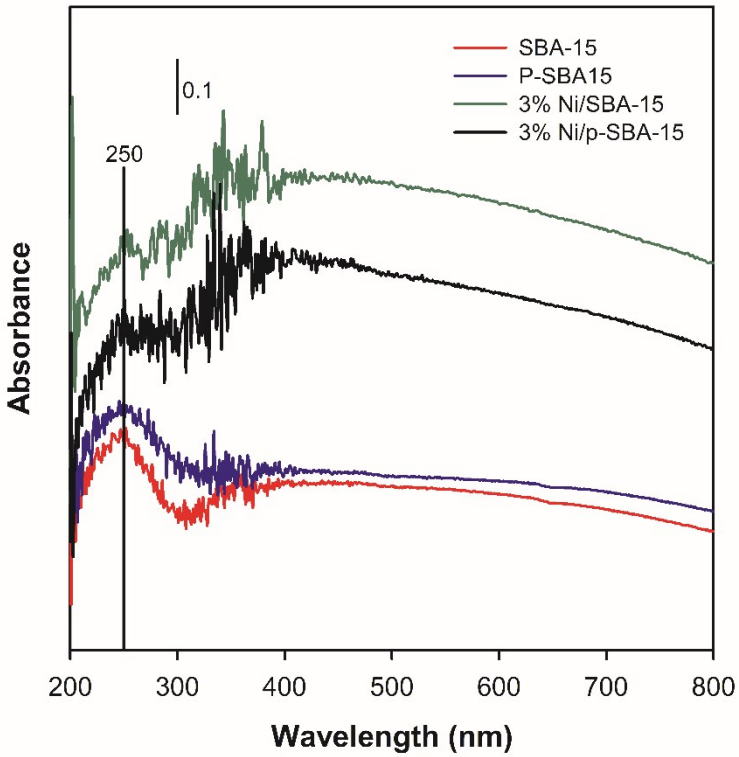


Fig. S15 UV-Vis spectra of SBA-15, p-SBA-15, 3% Ni/p-SBA-15 and 3% Ni/SBA-15 samples.

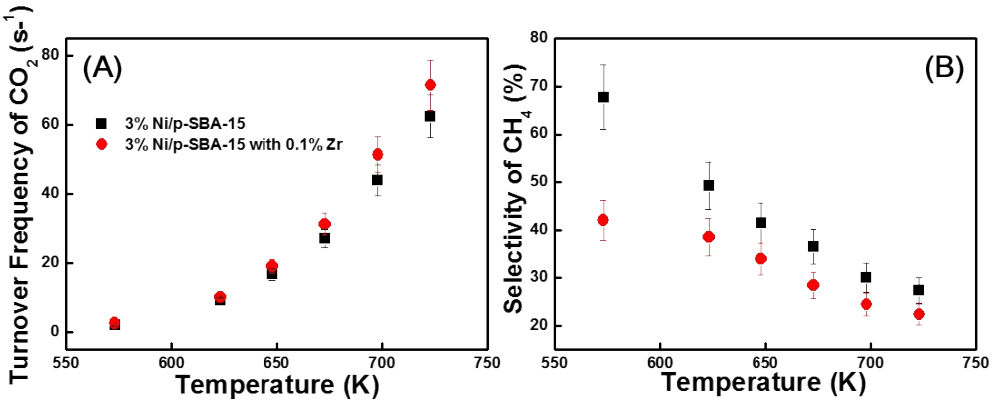


Fig. S16 Temperature-dependent $CO_2$ hydrogenation on 3 wt% Ni/p-SBA-15 with and without 0.1 wt% Zr additives. A $H_2/CO_2$ stream (1:1 ratio) with a 100 mL $min^{-1}$ flow rate was passed over 10 mg of the catalyst. The GHSV was 600,000 $cm^3g^{-1}h^{-1}$.